

FITTING INFINITELY DIVISIBLE DISTRIBUTION: CASE OF GAMMA-VARIANCE MODEL

A.H.NZOKEM¹

ABSTRACT. The paper examines the Fractional Fourier Transform (FRFT) based technique as a tool for obtaining the probability density function and its derivatives; and mainly for fitting stochastic model with the fundamental probabilistic relationships of infinite divisibility. The probability density functions are computed and the distributional proprieties such as leptokurtosis, peakedness, and asymmetry are reviewed for Variance-Gamma (VG) model and Compound Poisson with Normal Compounding model. The first and second derivatives of probability density function of the VG model are also computed in order to build the Fisher information matrix for the Maximum likelihood method.

The VG model has been increasingly used as an alternative to the Classical Lognormal Model (CLM) in modelling asset price. The VG model with five parameters was estimated by the FRFT. The data comes from the daily SPY ETF price data. The Kolmogorov-Smirnov (KS) goodness-of-fit shows that the VG model fits better the empirical cumulative distribution than the CLM. The best VG model comes from the FRFT estimation.

Infinitely divisible distributions, Variance Gamma (VG) Model, Classical Lognormal Model (CLM), Fractional Fourier Transform (FRFT), Maximum likelihood, Function Characteristic, SPDR S&P500 ETF (SPY), Kolmogorov-Smirnov (K-S)

1. INTRODUCTION

Empirical studies have shown that asset returns are often characterized by peakedness, leptokurtosis and asymmetry. Most of these empirical properties were reviewed in [1] as a set of stylized empirical facts that emerge from price variations in various types of financial markets. These facts provide evidence suggesting the assumptions of the Classical Lognormal Model (CLM) are not consistent with the empirical observations. In order to reduce the theoretical-empirical gap, it has been used in literature two sophisticated stochastic processes with the fundamental probabilistic relationships of infinite divisibility. A natural generalization of the Brownian motion, which is the Lévy process. As a stochastic process, the Lévy process has independent and stationary increments; and as a function, the process is right continuous with left limit. However, the Lévy process model is usually incomplete, as the associated risk-neutral equivalent martingale measure is usually not unique; and this situation leads to many different possible prices for European options [2, 3].

Another way to generalize the Classical Lognormal Model (CLM) is the method of subordination [3–5]. The subordinated process is obtained by substituting the physical time in the CLM by any independent and stationary increments random process, called the subordinator. If we consider the random process to be a Gamma process, we have a Variance Gamma (VG) model,

¹ hilaire77@gmail.com.

which is the model the paper will be investigating. The Variance Gamma (VG) model was proposed by [6] as an alternative to the Classical Lognormal Model (CLM). In contrast to the CLM, the VG model does not have an explicit closed-form for probability density function and its derivatives. However, the fundamental probabilistic relationship of infinite indivisibility allows the characteristic function of the VG model and the Fourier of probability density function to have a closed-form function. In the study, the VG model has five parameters: parameters of location (μ), symmetric (δ), volatility (σ), and the Gamma parameters of shape (α) and scale (θ). The VG model density function is proven to be (1.1).

$$f(y) = \frac{1}{\sigma\Gamma(\alpha)\theta^\alpha} \int_0^{+\infty} \frac{1}{\sqrt{2\pi v}} e^{-\frac{(y-\mu-\delta v)^2}{2v\sigma^2}} v^{\alpha-1} e^{-\frac{v}{\theta}} dv \quad (1.1)$$

The integral in (1.1) makes it difficult to utilize the density function and its derivatives, and to perform the Maximum likelihood method. However, in the literature, many studies have found a way to circumvent the lack of closed-form by decreasing the number of parameters and making use of approximation function or analytical expression with modified second kind Bessel function. In fact, [7] developed a procedure to approximate (1.1) by Chebyshev Polynomials expansion. [8] and [9] got (1.1) by analytical expression with modified Bessel function of second kind and third kind respectively. [3] got (1.1) through Gauss-Laguerre quadrature approximation with Laguerre polynomial of degree 10. [5] used the Fast Fourier Transform (FFT).

The paper will implement the Fractional Fourier Transform (FRFT)-based technique on the Fourier Transform of the VG model function in order to obtain probability density function and its derivatives. Contrary to the Fast Fourier Transform (FFT), the advantage of using the FRFT mentioned in [10] can be found at three levels: (1) both the input function values and the output transform function values are equally spaced; (2) a large fraction of the density function is either zero or smaller than the computer machine epsilon; and (3) only a limited range of the density function are required.

The paper is structured as follows, the next section presents the analytical framework, with an overview of the FRFT computing formulas, their applications on three infinitely divisible distributions, and a review of the Maximum likelihood method. The third section will present the Variance Gamma (VG) model and the sample data, before performing the parameter estimations of the VG model and the Kolmogorov-Smirnov (KS) goodness-of-fit test.

2. ANALYTICAL FRAMEWORK

The continuous Fourier transform (CFT) of function $f(t)$ and its inverse are defined by:

$$\mathcal{F}[f](x) = \int_{-\infty}^{+\infty} f(y) e^{-ixy} dy \quad (2.1)$$

$$f(x) = \frac{1}{2\pi} \int_{-\infty}^{+\infty} \mathcal{F}[f](y) e^{ixy} dy \quad (2.2)$$

where i is the imaginary unit.

The Fast Fourier Transform (FFT) is commonly used to evaluate the integrals (2.1) and (2.2). The fundamentally inflexible nature [10] of FFT is the main weakness of the algorithm. The advantages of computing with the FRFT mentioned in [10] can be found at three levels: (1) both the input function values $f(x_k)$ and the output transform values $\mathcal{F}[f](x_k)$ are equally spaced; (2)

a large fraction of $f(x_k)$ are either zero or smaller than the computer machine epsilon; and (3) only a limited range of $f(x_k)$ are required.

The FRFT is set up on n -long sequence (x_1, x_2, \dots, x_n) by:

$$G_k(x, \delta) = \sum_{j=0}^{n-1} x_j e^{-2\pi i j k \delta} \quad 0 \leq k < M \quad (2.3)$$

For $\delta = \frac{1}{n}$, we have the Discrete Fourier Transform (DFT). In the general scheme, the parameter δ is not limited to fractions; it can take complex number. It is shown in [11] that $G_k(x, \delta)$ is a composition of DFT^{-1} and DFT .

$$G_k(x, \delta) = e^{-\pi i k^2 \delta} DFT_k^{-1}[DFT_j(y) DFT_j(z)] \quad (2.4)$$

where y and z are two $2n$ -long sequences defined by:

$$y_j = e^{-2\pi i j^2 \delta} \quad z_j = e^{-2\pi i j^2 \delta} \quad 0 \leq k < n \quad (2.5)$$

$$y_j = 0 \quad z_j = e^{-2\pi i (j-2m)^2 \delta} \quad n \leq k < 2n \quad (2.6)$$

As shown in (2.4), the FRFT is efficiently computed through the FFT on $2n$ -point. We assume that $\mathcal{F}[f](t)$ is zero outside the interval $[-\frac{a}{2}, \frac{a}{2}]$, and $\beta = \frac{a}{n}$ is the step size of the n input values $\mathcal{F}[f](t)$; we define $t_j = (j - \frac{n}{2})\beta$ for $0 \leq j < n$. We have also γ as the step size of the n output values of $f(t)$ and $x_k = (k - \frac{n}{2})\gamma$ for $0 \leq k < n$. By choosing the step size β on the input side and the step size γ in the output side, we fix the FRFT parameter $\delta = \frac{\beta\gamma}{2\pi}$.

The density function f at x_k can be written as (2.7). The proof is provided in Appendix A.1.

$$\hat{f}(x_k) = \frac{\gamma}{2\pi} e^{-\pi i (k - \frac{n}{2}) n \delta} G_k(\mathcal{F}[f](y_j) e^{-\pi i j n \delta}), -\delta) \quad (2.7)$$

In order to perform $f(t)$ function from the Fourier Transform (FT), we assume $a = 20$, $n = 2048$, $\beta = \gamma = \frac{a}{n}$. For more detail on FRFT, See [10], [11].

2.1 Infinitely Divisible Distributions.

The FRFT probability density functions are computed for each of the three infinitely divisible distributions: Normal distribution with two parameters, Variance Gamma (VG) Distribution with five parameters, and Compound Poisson with Normal compounding with three parameters. The distributional properties are reviewed and the results also show that the Kurtosis statistics tell very little about the peakedness [12].

For detailed proof of infinite divisibility for each distribution. See [13], [14], [15]

2.1.1 Normal distribution.

$$X \sim \mu + N(0, \sigma^2)$$

The normal distribution is an infinitely divisible distribution. It was shown in [13] that the normal distribution $N(\mu, \sigma)$ is the n^{th} convolution power of a probability measure $N(\frac{\mu}{n}, \frac{\sigma}{n})$, for every n . The density and the Fourier transform functions have an explicit closed form as shown below.

$$\mathcal{F}[f](x) = e^{-uix - \frac{1}{2}\sigma^2 x^2} \quad (2.8)$$

$$f(x) = \frac{1}{\sigma\sqrt{2\pi}} e^{-\frac{(y-\mu)^2}{2\sigma^2}} \quad (2.9)$$

For mean ($\mu = -2$) and standard deviation ($\sigma = 1$), Fig 1a displays the FRFT estimation of the Normal density function and Fig 1b shows the absolute value between the estimations and the exact values of the normal density function.

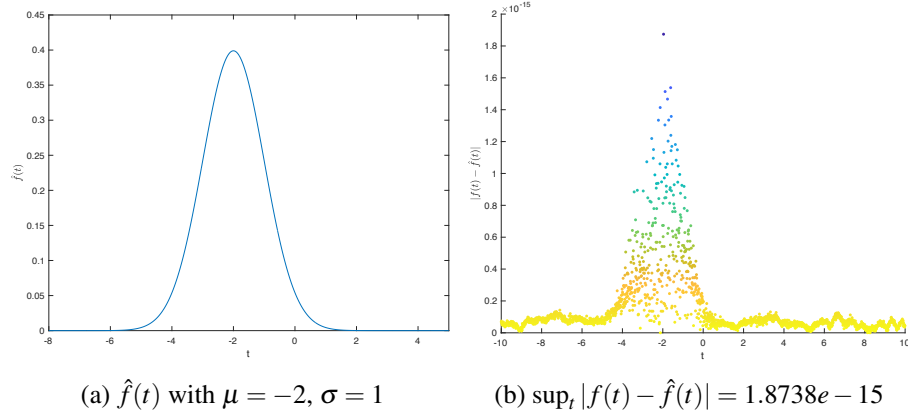


FIGURE 1. FRFT estimation of the Normal density function

The highest computation error is $1.8738e - 15$, which is negligible. The probability density function is symmetric with the Kurtosis statistic 3 for the normal distribution.

2.1.2 Variance Gamma (VG) Distribution.

$$X = \mu + \gamma V + \sigma \sqrt{V} Z$$

$$Z \sim N(0, 1) \quad \text{and} \quad V \sim \Gamma(\alpha, \theta)$$

The Variance Gamma distribution is an infinitely divisible distribution. The density function is (2.11) and does not have a closed form. However, the Fourier transform function has explicit closed form (2.10). See Appendix A.1 for proof

$$\mathcal{F}[f](x) = \frac{e^{-i\mu x}}{\left(1 + \frac{1}{2}\theta\sigma^2 x^2 + i\gamma\theta x\right)^\alpha} \quad (2.10)$$

$$f(y) = \frac{1}{\sigma\Gamma(\alpha)\theta^\alpha} \int_0^{+\infty} \frac{1}{\sqrt{2\pi v}} e^{-\frac{(y-\mu-\delta v)^2}{2v\sigma^2}} v^{\alpha-1} e^{-\frac{v}{\theta}} dv \quad (2.11)$$

When $\delta = 0$, we have Symmetric Variance Gamma (SVG) Model, which is a special case of the Variance Gamma (VG) Model. It can be shown through Cumulant-generating function [16] that

$$E(X) = \mu \quad \text{Var}(X) = \alpha\theta\sigma^2 \quad \text{Skew}(X) = 0 \quad \text{Kurt}(X) = 3\left(1 + \frac{1}{\alpha}\right) \quad (2.12)$$

For Parameter values: $\mu = -2, \delta = 0, \sigma = 1, \alpha = 1, \theta = 1$. Fig 2 displays the FRFT estimation of the probability density functions. As shown in Fig 2b, the probability density is left asymmetric and right asymmetric when the parameter (δ) is negative and positive respectively. For $\delta = 0$, the density function is symmetric, as shown in (2.12). The shape parameter (α) impacts the peakedness and tails of the distribution, as illustrated in Fig 2c and (2.12); heavier is the tails, shorter is the peakedness. θ and σ have the same impact on the distribution. As shown in (2.12), both change only the variance.

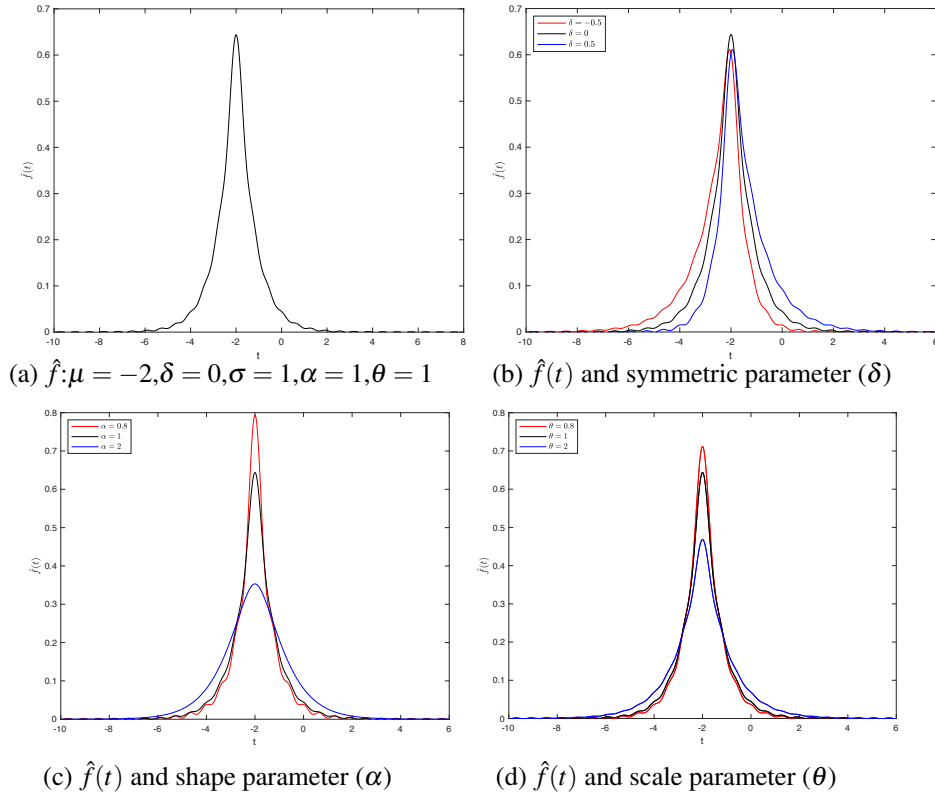


FIGURE 2. FRFT estimation of the Variance Gamma density function

2.1.3 Compound Poisson with Normal Compounding.

$$X = \sum_{i=1}^{N(\lambda)} X_j$$

$$N(\lambda) \sim \text{Poisson}(\lambda) \quad \text{and} \quad X_j \sim \mu + N(0, \sigma^2)$$

The density function was shown in [17] to be (2.14). However, the Fourier Transform density has explicit closed form (2.13). See Appendix A.1 for proof.

$$\mathcal{F}[f](x) = e^{\lambda(e^{-i\mu x - \frac{1}{2}\sigma^2 x^2} - 1)} \quad (2.13)$$

$$f(x) = \sum_{n=1}^{\infty} \frac{e^{-\lambda} \lambda^n}{n!} \frac{e^{-\frac{1}{2} \frac{(x-n\mu)^2}{n\sigma^2}}}{\sigma \sqrt{2n\pi}} \quad (2.14)$$

It can be shown through Cumulant-generating function [16] that

$$E(X) = \lambda\mu \quad \text{Var}(X) = \lambda(\mu^2 + \sigma^2) \quad \text{Skew}(X) = \frac{\mu(\mu^2 + 3\sigma^2)}{\sqrt{\lambda}(\mu^2 + \sigma^2)^{\frac{3}{2}}} \quad \text{Kurt}(X) = 3 + \frac{\mu^4 + 6\sigma^2\mu^2 + 3\sigma^4}{\lambda(\mu^2 + \sigma^2)^2} \quad (2.15)$$

For Parameter values: $\mu = -0.1$, $\sigma = 0.25$, $\lambda = 16$. The FRFT produces the density functions in Fig 3. As shown in Fig 3b, the probability density is asymmetric, shifts to the left and to the right when the parameter (μ) is negative and positive respectively. For $\mu = 0$, we have a symmetric

density function. μ and σ impact the symmetry, peakedness and tails of the distribution, as illustrated in Fig 3c and (2.15); heavier is the tails, shorter is the peakedness. The Poisson parameter (λ) impacts all the statistics in (2.15). λ affects the asymmetry, peakedness and tails of the distribution simultaneously.

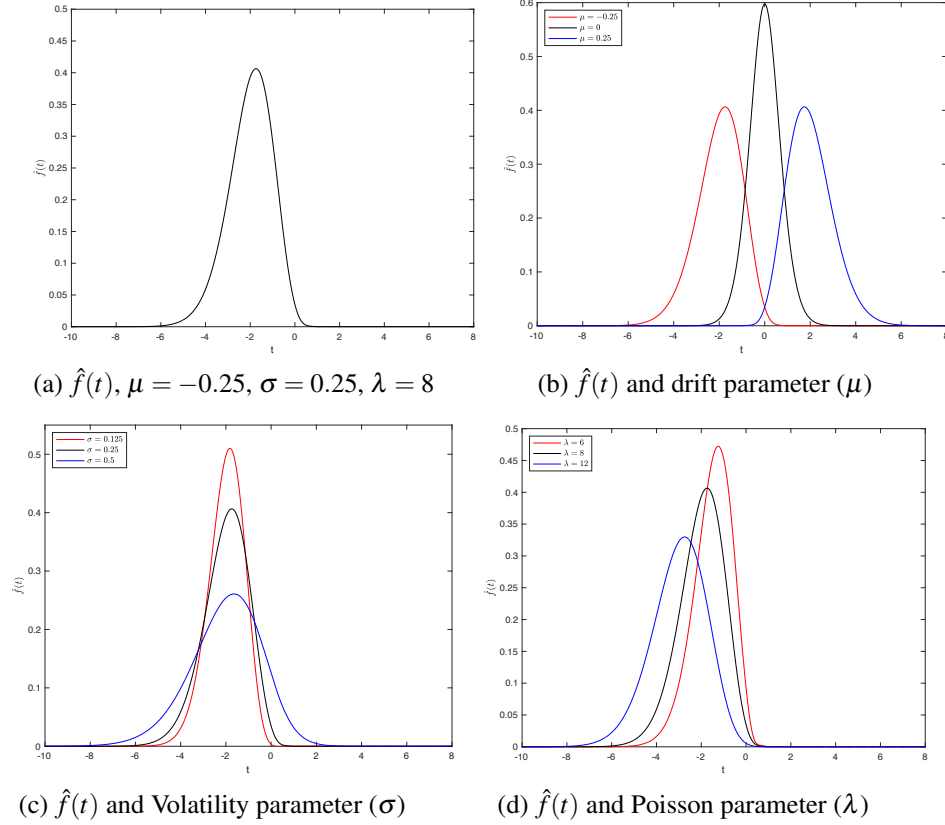


FIGURE 3. FRFT estimation of the Compound Poisson with Normal Compounding density function

2.2 Review of the Maximum Likelihood Method.

From a probability density function $f(x, V)$ with parameter V of size p and the sample data x of size m , we define the Likelihood Function as shown in (2.16).

$$L(x, V) = \prod_{j=1}^m f(x_j, V) \quad (2.16)$$

$$l(x, V) = \sum_{j=1}^m \log(f(x_j, V)) \quad (2.17)$$

$$\frac{dl(x, V)}{dV_j} = \sum_{i=1}^m \frac{\frac{df(x_i, V)}{dV_j}}{f(x_i, V)} \quad 1 \leq j \leq p \quad (2.18)$$

$$\frac{d^2l(x, V)}{dV_k dV_j} = \sum_{i=1}^m \left(\frac{\frac{d^2f(x_i, V)}{dV_k dV_j}}{f(x_i, V)} - \frac{\frac{df(x_i, V)}{dV_k}}{f(x_i, V)} \frac{\frac{df(x_i, V)}{dV_j}}{f(x_i, V)} \right) \quad 1 \leq k \leq p \text{ and } 1 \leq j \leq p \quad (2.19)$$

In order to perform the Maximum of the likelihood function (2.16), the quantities $\frac{dl(x, V)}{dV_j}$ and $\frac{d^2l(x, V)}{dV_k dV_j}$ must be computed. We need to compute $\frac{df(x, V)}{dV_j}$ and $\frac{d^2f(x, V)}{dV_k dV_j}$, which are the first and second order derivative of the density function respectively. Variance Gamma (VG) distribution has five parameters (μ , δ , σ , α , θ), using the closed form of Fourier transform in (2.10) and the FRFT algorithm, we perform the first derivative functions: $\frac{df}{d\mu}$, $\frac{df}{d\delta}$, $\frac{df}{d\sigma}$, $\frac{df}{d\alpha}$ and $\frac{df}{d\theta}$. The results of the computation are shown in Fig 4.

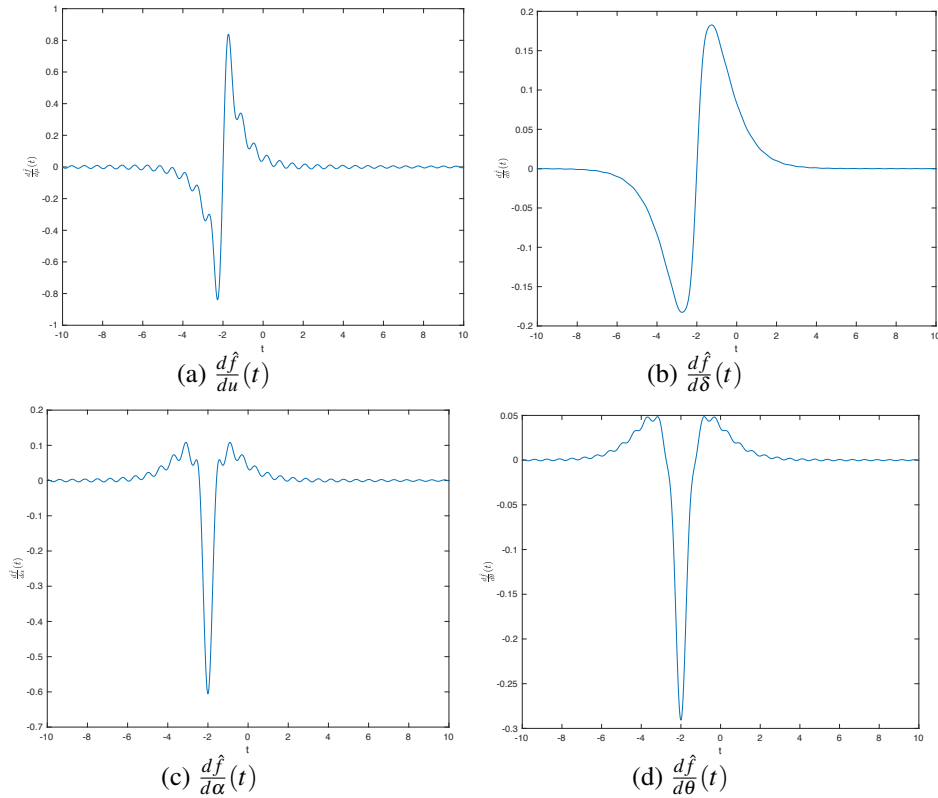


FIGURE 4. First order derivative of VG density function with $\mu = -2$, $\delta = 0$, $\sigma = 1$, $\alpha = 1$, $\theta = 1$

As shown in Fig 4, we have two Odd functions in Fig 4a and 4b generated by the drift parameters μ and δ ; and the remainings are Even functions. The functions in Fig 4c, and Fig 4d are symmetric along the vertical line $x = -2$, whereas $\frac{df(x, V)}{d\mu}$ and $\frac{df(x, V)}{d\delta}$ have rotational symmetry at the point $(-2, 0)$. In addition, each graph has positive area values and negative

area values. Having such properties is a necessary condition to find $V(\mu, \delta, \sigma, \alpha, \theta)$ such as $(\frac{dl(x,v)}{d\mu}, \frac{dl(x,v)}{d\delta}, \frac{dl(x,v)}{d\sigma}, \frac{dl(x,v)}{d\alpha}, \frac{dl(x,v)}{d\theta})$ equals zero.

The quantities $\frac{d^2l(x,V)}{dV_i dV_j}$ in (2.19) are critical in computing the Hessian Matrix and the Fisher Information Matrix. For VG distribution, We need fifteen second derivative functions. The results of four functions are shown in Fig 5. The remaining functions are reported in Appendix B.2 and Appendix C.3.

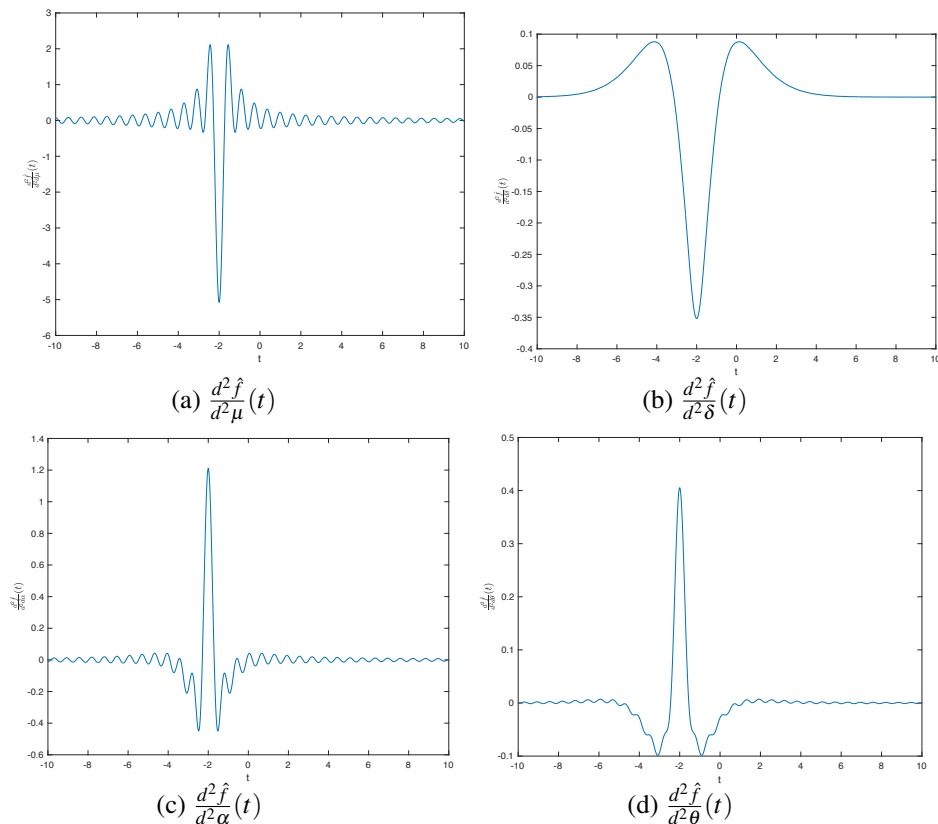


FIGURE 5. Second order derivative of VG density function with $\mu = -2$, $\delta = 0$, $\sigma = 1$, $\alpha = 1$, $\theta = 1$

As shown in Fig 5, all four functions are symmetric along the vertical line $x = -2$. We have the same characteristics for $\frac{d^2 \hat{f}}{d\delta d\mu}$, $\frac{d^2 \hat{f}}{d^2 \sigma}$, $\frac{d^2 \hat{f}}{d\alpha d\sigma}$, $\frac{d^2 \hat{f}}{d\theta d\sigma}$, $\frac{d^2 \hat{f}}{d\theta d\alpha}$ in Appendix B.2 and Appendix C.3. The remaining derivatives have rotational symmetry at the point $(-2, 0)$. These features can be checked analytically through the Inverse Fourier Transform in (2.2) and $\mathcal{F}[f]$ in (2.10).

Given the parameters $V(\mu, \delta, \sigma, \alpha, \theta)$ and the sample data set x , from the previous development and computations, we have the quantities:

$$l'(x, V) = \left(\frac{dl(x, V)}{d\mu}, \frac{dl(x, V)}{d\delta}, \frac{dl(x, V)}{d\sigma}, \frac{dl(x, V)}{d\alpha}, \frac{dl(x, V)}{d\theta} \right) \quad (2.20)$$

$$I''(x, V) = \begin{bmatrix} \frac{d^2 l}{d^2 \mu} & \frac{d^2 l}{d\delta d\mu} & \frac{d^2 l}{d\sigma d\mu} & \frac{d^2 l}{d\alpha d\mu} & \frac{d^2 l}{d\theta d\mu} \\ \frac{d^2 l}{d\delta d\mu} & \frac{d^2 l}{d^2 \delta} & \frac{d^2 l}{d\sigma d\delta} & \frac{d^2 l}{d\delta d\alpha} & \frac{d^2 l}{d\theta d\delta} \\ \frac{d^2 l}{d\sigma d\mu} & \frac{d^2 l}{d\sigma d\delta} & \frac{d^2 l}{d^2 \sigma} & \frac{d^2 l}{d\alpha d\sigma} & \frac{d^2 l}{d\theta d\sigma} \\ \frac{d^2 l}{d\alpha d\mu} & \frac{d^2 l}{d\alpha d\delta} & \frac{d^2 l}{d\alpha d\sigma} & \frac{d^2 l}{d^2 \alpha} & \frac{d^2 l}{d\theta d\alpha} \\ \frac{d^2 l}{d\theta d\mu} & \frac{d^2 l}{d\theta d\delta} & \frac{d^2 l}{d\theta d\sigma} & \frac{d^2 l}{d\alpha d\theta} & \frac{d^2 l}{d^2 \theta} \end{bmatrix} \quad (2.21)$$

$I'(x, V)$ is the score function with the property [18] that $E(I'(x, V)) = 0$. $-I''(x, V)$ is the observed Fisher information and $I(V) = E(I''(x, V))$ is the Fisher information matrix. Maximizing $L(x, V)$ in (2.16) with respect to V is equivalent to solving the equation system (2.22).

$$I'(x, V) = 0 \quad (2.22)$$

The solutions of (2.22) are provided by the Newton–Raphson Iteration Algorithm (2.23). In fact, the *Taylor's* expansion can be applied to the score function to derive the Newton–Raphson Iteration Algorithm.

$$V^{n+1} = V^n + (I''(x, V^n))^{-1} I'(x, V^n) \quad (2.23)$$

For more detail on Maximum likelihood and Newton–Raphson Iteration procedure, see [18], [19], [20], [21], [22].

3. FITTING VARIANCE GAMMA (VG) MODEL

3.1 VG Model and Asset/Index price.

The VG model was introduced by Madan et al [6, 9]. The idea [23] was to model the asset price on bussiness time rather than on calender time. The asset price is modelled on bussiness time (k) as follows:

$$Y_k = \mu + \delta V_k + \sigma \sqrt{V_k} Z \quad Z \sim N(0, 1) \quad V_k \sim \Gamma(\alpha, \theta) \quad (3.1)$$

$$S_K = S_{k-1} e^{\sum_{j=k}^K Y_j} \quad T_K = \sum_{k=1}^K V_k \quad (3.2)$$

Where $\mu, \delta \in R$, $\sigma > 0$, $\alpha > 0$ and $\theta > 0$. μ is the drift of the physical time scale, δ is the drift of the activity time process, and σ is the volatility. $\{T_k\}$ is the activity time process [24] or intrinsic time process [5] and is supposed to be non-negative stationary independent increments. This process is associated with either the flow of new price-sensitive information or the cumulative trading volume process. Y_k is the return variable of the stock or index price, we have (3.3) from (3.1) and (3.2).

$$Y_k = \log\left(\frac{S_k}{S_{k-1}}\right) \quad E(Y_k | V_k) \sim N(\mu + \delta V_k, V_k \sigma^2) \quad V_k \sim \Gamma(\alpha, \theta) \quad (3.3)$$

The density of Y_j in (3.1) and (3.3) has the following expression

$$f(y) = \frac{1}{\sigma\Gamma(\alpha)\theta^\alpha} \int_0^{+\infty} \frac{1}{\sqrt{2\pi v}} e^{-\frac{(y-\mu-\delta v)^2}{2v\sigma^2}} v^{\alpha-1} e^{-\frac{v}{\theta}} dv \quad (3.4)$$

The Fourier transform of (3.4) can be shown to be .

$$F[f](x) = E[e^{-ixY_j}] = \frac{e^{-i\mu x}}{\left(1 + \frac{1}{2}\theta\sigma^2 x^2 + i\delta\theta x\right)^\alpha} \quad (3.5)$$

See A.1 for proof (3.5).

For $\alpha = \frac{1}{\theta}$ and $0 < \theta \ll 1$, Y_k in (3.1) becomes

$$Y_k \sim N(\mu + \delta, \sigma^2) \quad (3.6)$$

See A.1 for proof (3.6)

The relationship between means ($E(Y_j)$), variance ($Var(Y_j)$), Skewness ($Skew(Y_j)$) and Kurtosis ($Kurt(Y_j)$) indicators and the VG model with five parameters can be shown by Cumulant-generating function [16].

$$E(Y_j) = \mu + \alpha\theta\delta \quad (3.7)$$

$$Var(Y_j) = \alpha(\delta^2\theta^2 + \theta\sigma^2) \quad (3.8)$$

$$Skew(Y_j) = \frac{\delta(2\delta^2 + 3\frac{\sigma^2}{\theta})}{\alpha^{\frac{1}{2}}(\delta^2 + \frac{\sigma^2}{\theta})^{\frac{3}{2}}} \quad (3.9)$$

$$Kurt(Y_j) = 3 \left(1 + \frac{2\delta^4 + \frac{\sigma^4}{\theta^2} + \frac{4\sigma^2\delta^2}{\theta}}{\alpha(\delta^2 + \frac{\sigma^2}{\theta})^2} \right) \quad (3.10)$$

By applying the method of Moments, the system of equations has more parameters than equations. The issue can be overcome by imposing [3] $E(V) = 1$ or $\sigma = 1$. $E(V) = 1$ was chosen in [9, 25] and the implication was that the gamma shape and scale parameters should be equal ($\alpha = \theta$). In the next section, we will assume $\sigma = 1$ in order to solve the system of equation (3.7)...(3.10). However, the constraints will be relaxed in the Maximum Likelihood method where all five VG parameters will be estimated.

3.2 data.

The data comes from the SPY ETF, called SPDR S&P 500 ETF (SPY). The SPY is an Exchange-Traded Fund (ETF) managed by State Street Global Advisors that tracks the Standard & Poor's 500 index (S&P 500), which comprises 500 large and mid-cap US stocks. The SPY is a well-diversified basket of assets, listed on the New York Stock Exchange (NYSE). Like other ETFs, SPY provides the diversification of a mutual fund and the flexibility of a stock.

The SPY data was extracted from Yahoo finance. The daily data was adjusted for splits and dividends. The period spans from January 4, 2010 to December 30, 2020. 2768 daily SPY ETF price was collected, around 252 observations per year, over 10 years. The dynamic of daily adjusted SPY price is provided in Fig 6.

As a whole, the SPY price has an increasing trend during the period 2010-2020. The increase is

temporally disrupted in the first quarter of 2020 by the coronavirus pandemic.

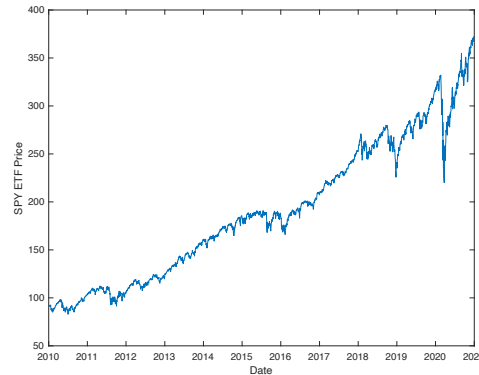
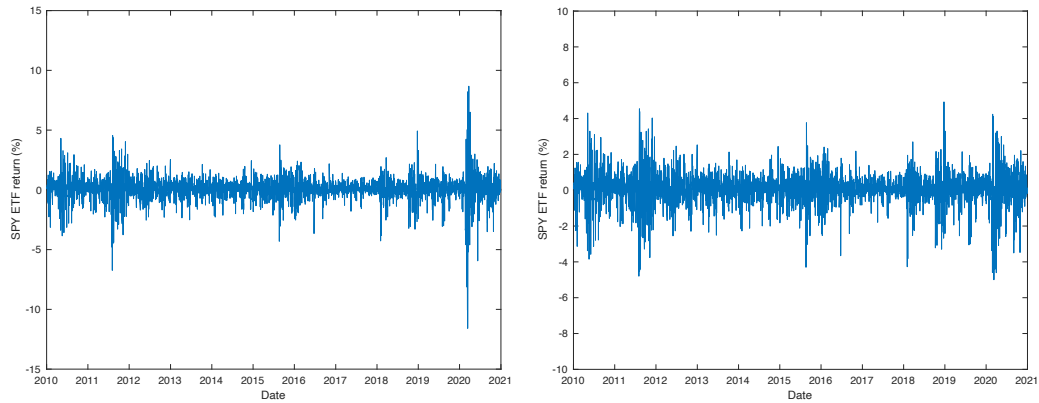


FIGURE 6. Daily SPY ETF Price

Let the number of observations $N = 2768$, and the daily observed SPY price S_j on day t_j with $j = 1, \dots, N$; t_1 is the first observation date (January 4, 2010) and t_N is the last observation date (December 30, 2020). The daily SPY ETF log return (y_j) is computed as in (3.11).

$$y_j = \log(S_j/S_{j-1}) \quad j = 2, \dots, N \quad (3.11)$$

One observation will be lost in the computation process. The results of the daily SPY ETF return are shown in Fig 7. The volatility of the SPY ETF is higher in the First quarter of 2020 as



(a) Daily SPY return and COVID-19 pandemic (b) Daily SPY return sample without outliers

FIGURE 7. Daily SPY ETF Return (%)

displayed in Fig 7a. The SPY ETF is an inexpensive way for investors to gain diversified exposure to the U.S. stock market; like others stocks and securities, it was unusually volatile in 2020 amid the coronavirus pandemic and massive disruptions in the global economy.

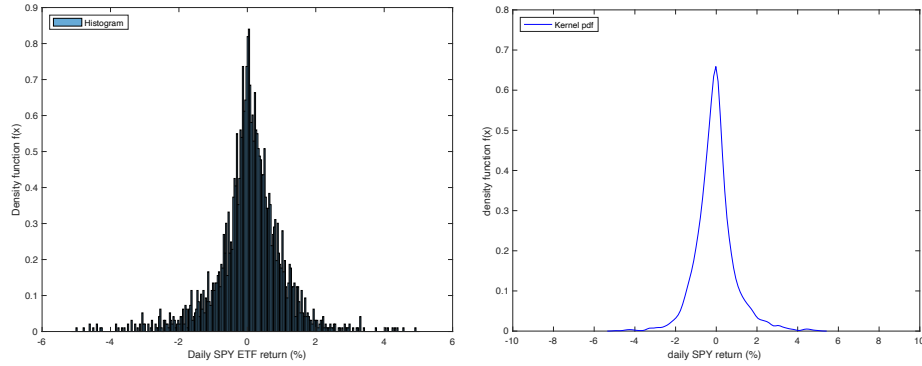
13 daily return observations was identified as outliers and removed from the data set in order to avoid negative impact on the statistics. See Table 1 below. By assuming the independent, identically distribution in the SPY ETF return sample, the method of moments was used to compute statistics in Table 1 for both samples with outliers and without outliers. The outlier effects are greater on Kurtosis, Skewness, and Variance. The sample Skewness (0.4687) is between -0.5 and

0.5, which is the skewness interval for symmetric [5, 26].

TABLE 1. Impact of outliers on sample Statistics

Statistics	All	Without outliers
N	2768	2755
$E(\hat{Y})$	0.0509	0.0541
$\sigma^2(\hat{Y})$	1.1905	0.9487
$Skew(\hat{Y})$	-0.8633	-0.4687
$Kurt(\hat{Y})$	17.3572	6.6853

The shape of the daily SPY ETF return distribution are estimated from the sample using two non parametric density estimators: Histogram in Fig 8a and Kernel density function in Fig8b. Both graphs show the Leptokurtosis [25] with sharp peak.



(a) Daily SPY ETF return Histogram (b) Daily SPY ETF return Kernel density

FIGURE 8. Non-parametric density estimation

3.3 VG Model Estimations.

Based on the VG model assumption that $\sigma = 1$, the equations (3.7)-(3.10) was solved given the statistics provided in Table 1. The parameter values μ , δ , α , and θ are shown in Table 2. We have two models, the asymmetric Variance-Gamma model (AVG) with chronometer drift negative ($\delta = -0.1399$); and the symmetric Variance-Gamma model (SVG) without drift.

As shown Table 2, when $\delta = 0$, the drift of the physical time scale μ decreases, but keeps the positive sign. The magnitude of α and θ remains the same. The Gamma shape parameter (α) is less than one. In fact, The larger the sample kurtosis, the smaller the Gamma shape parameter (α) as shown in the relationship ($Kurtosis = 3(1 + \frac{1}{\alpha})$) for SVG model.

TABLE 2. Method of Moments VG Parameters Estimations

Model	Parameters	Statistics
AVG	$\hat{\mu} = 0.1841$	$Skew(Y) = -0.4689$
	$\hat{\delta} = -0.1399$	
	$\hat{\alpha} = 0.8479$	$Kurt(Y) = 6.6853$
	$\hat{\theta} = 1.0954$	
SVG	$\hat{\mu} = 0.0541$	$Skew(Y) = 0$
	$\hat{\alpha} = 0.8140$	$Kurt(Y) = 6.6853$
	$\hat{\theta} = 1.1654$	

Regarding the estimation by Maximum likelihood method, the previous assumption on the volatility ($\sigma = 1$) does not hold and was dropped. The method has a local property that makes the result depending on the initial value. The estimations by Moments method were used as initial values in the maximization procedure.

TABLE 3. Maximum Likelihood VG Parameters Estimations

Model	Parameters	Statistics
AVG1	$\hat{\mu} = 0.1683$	$Skew(Y) = -0.382$
	$\hat{\delta} = -0.1089$	$Kurt(Y) = 6.329$
	$\hat{\sigma} = 0.8987$	$Log(ML) = -3562$
	$\hat{\alpha} = 0.9284$	$P_value = 0$
	$\hat{\theta} = 1.0546$	
SVG1	$\hat{\mu} = 0.0510$	$Skew(Y) = 0$
	$\hat{\sigma} = 0.9378$	$Kurt(Y) = 6.534$
	$\hat{\alpha} = 0.8490$	$Log(ML) = -3559$
	$\hat{\theta} = 1.0929$	$P_value = 0$
AVG2	$\hat{\mu} = 0.0848$	$Skew(Y) = -0.173$
	$\hat{\delta} = -0.0577$	$Kurt(Y) = 6.412$
	$\hat{\sigma} = 1.0295$	$Log(ML) = -3548.65$
	$\hat{\alpha} = 0.8845$	$P_value = 0$
	$\hat{\theta} = 0.9378$	
SVG2	$\hat{\mu} = 0.0652$	$Skew(Y) = 0$
	$\hat{\sigma} = 0.9939$	$Kurt(Y) = 6.421$
	$\hat{\alpha} = 0.8770$	$Log(ML) = -3552.29$
	$\hat{\theta} = 0.9937$	$P_value = 0$
CLM	$\hat{\mu} = 0.0541$	$Kurt(Y) = 3$
	$\hat{\sigma} = 0.9740$	$Log(ML) = -3836.16$

In table 3, the results are labeled AVG1 for the Asymmetric Variance-Gamma Model and SVG1 for the Symmetric Variance-Gamma Model. Another initial value was chosen with $\sigma = \alpha = \theta = 1$, and $\delta = \mu = 0$. The results are labeled AVG2 and SVG2 respectively for Asymmetric Variance-Gamma Model and Symmetric Variance-Gamma Model. As shown in Appendix D.4, the maximization procedure convergences after 21 iterations For AVG2, as shown in Table 5. SVG2 also converges, after 15 iterations. See Table 6 in Appendix D.4.

It appears that the drift of the physical time scale μ is positive, and the drift of the activity time process δ is negative. The estimation of the Maximum likelihood underestimates the value of the kurtosis.

3.4 Comparison of VG Models.

For the Classical Lognormal Model (CLM), the Method of Moments and the Maximum likelihood yield the same estimation of the mean ($\hat{\mu}$) and standard deviation ($\hat{\sigma}$), given a high sample size. The results are displayed in Table 3.

It is shown in (3.3) that the VG model is a special case of the CLM. It is also known that the parameter values in Table 3 maximized the likelihood function. Therefore, it becomes appropriate to perform the Likelihood Ratio test between the normal distribution and the four other VG models. The Likelihood Ratio estimator (W) is defined as follows.

$$W = 2(L_{H_1} - L_{H_0}) \quad W \sim \chi^2(r) \quad P_value = \text{prob}(\chi^2 > \hat{W} | H_0) \quad (3.12)$$

where L_{H_0} is the Maximum of the Log-likelihood under H_0 . Under $H_0: Y_k \sim N(\mu, \sigma^2)$. L_{H_1} is the Maximum of the Log-likelihood under H_1 . Under $H_1: Y_k \sim VG(\mu, \delta, \sigma, \alpha, \theta)$. P_values is the probability that the real values are even more extreme (more in the tail) than our test statistic (\hat{W}). For Likelihood Ratio test review, see section 5.5 in [22], and [20], [27]

The value of the Log-likelihood ($Log(ML)$) is displayed in Table 3 for each model. There is a huge discrepancy between the Log-likelihood of the CLM and VG model, which produces P_value almost zero. Therefore, the null hypothesis (H_0) of normal distribution, is rejected based on the sample data. The results provide evidence that the Variance-Gamma model is an improvement compare to the classical Normal model.

The natural question is to know which VG model fits the empirical distribution of the sample of daily SPY ETF return $\{y_1, y_2 \dots y_n\}$. In order to compare the empirical distribution to the VG model theoretical distribution, the Kolmogorov-Smirnov (KS) test was performed under the null hypothesis (H_0) that the sample $\{y_1, y_2 \dots y_n\}$ comes from VG model.

The cumulative distribution function of the theoretical distribution needs to be computed. The density function (f) does not have closed-form, the same for the cumulative function (F) in (3.14). However, we know the closed form of the Fourier of the density function ($\mathcal{F}[f]$) and the relationship in (3.15) provides the Fourier of the cumulative distribution function ($\mathcal{F}[F]$).

$$Y \sim VG(\mu, \delta, \sigma, \alpha, \theta) \quad (3.13)$$

$$F(x) = \int_{-\infty}^x f(t) dt \quad f \text{ is the density function of } Y \quad (3.14)$$

$$\mathcal{F}[F](x) = \frac{\mathcal{F}[f](x)}{ix} + \pi \mathcal{F}[f](0) \delta(x) \quad (3.15)$$

$$\delta(x) = \begin{cases} 0 & \text{if } x \neq 0 \\ \infty & \text{if } x = 0 \end{cases} \quad (3.16)$$

See Appendix A.1 for (3.15) proof.

The cumulative distribution function (F) was computed from the inverse of the Fourier of the cumulative distribution ($\mathcal{F}[F]$). The results for SVG2 model is shown in Appendix E.5, Fourth column. The same methodology was followed for the remaining VG models. The Kolmogorov-Smirnov (K-S) estimator (D_n) is defined as follows.

$$D_n = \sup_x |F(x) - F_n(x)| \quad P_{value} = \text{prob}(D_n > d_n | H_0) \quad (3.17)$$

where n is the sample size, $F_n(x)$ denotes the empirical cumulative distribution of $\{y_1, y_2 \dots y_n\}$. The distribution of the Kolmogorov's goodness-of-fit measure D_n has been studied extensively in the literature [28], [29], [30]. It was shown that D_n distribution is independent of the theoretical distribution (F) under the null hypothesis (H_0). More recently in [31], it was determined numerically the exact distribution of D_n . [31] also provides a package `KSgeneral` [32] in the R software for computing the cumulative distribution of D_n when $F(x)$ is continuous and n is a natural number.

The cumulative distribution of D_n under the null hypothesis was computed and the density function was deduced. The computed density function is shown in Fig 9. Under the null hypothesis (H_0), D_n has a positively skewed distribution with means ($\mu = 0.0165$) and standard deviation ($\sigma = 5 * 10^{-3}$).

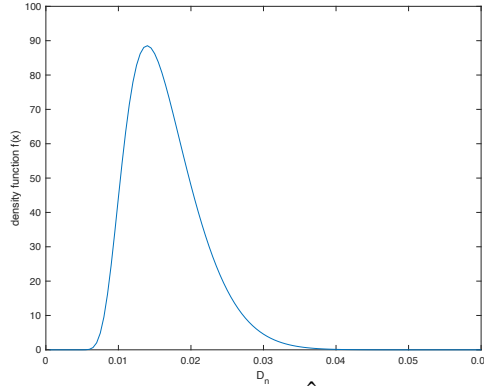


FIGURE 9. Kolmogorov-Smirnov Estimator (\hat{D}_n) probability density ($n = 2755$) under the null hypothesis H_0

d_n is the value of the KS estimator (D_n) computed from the sample $\{y_1, y_2 \dots y_n\}$. Based on [33, 34], d_n can be estimated as follows.

$$d_n^+ = \sup_{0 \leq j \leq P} |F(x_j) - F_n(x_j)| \quad d_n^- = \sup_{1 \leq j \leq P} |F(x_j) - F_n(x_{j-1})| \quad d_n = \text{Max}(d_n^+, d_n^-) \quad (3.18)$$

The results for SVG2 model is shown in Appendix E.5, Table E.5, Fifth and Sixth columns. From the Appendix E.5: $d_n^- = \text{max}((1)) = 0.023629$, $d_n^+ = \text{max}((2)) = 0.021986$ and $d_n = 0.023629$. For each estimation method and VG model, KS-Statistics (d_n) and P_values were computed and the results are provided in Table 4.

TABLE 4. Kolmogorov-Smirnov (KS) test

Method	Model	KS-Statistics (d_n)	P_values
Moments	SVG	0.058145	0.00000154%
	AVG	0.027211	3.3191%
	AVG1	0.054290	0.00001691%
Likelihood	SVG1	0.036763	0.1136%
	AVG2	0.028182	2.4668%
	SVG2	0.023629	9.0788%
	CLM	0.095791	0%

As shown in Table 4, the VG models from the method of moments do not fit the sample data distribution. The P_values is less than 5% and the null hypothesis H_0 can not be accepted at some extent. The CLM does not fit the sample data distribution at 5%. Regarding the maximum likelihood method, the SVG2 model has $P_values = 9.079\%$, which is high than the classical threshold 5%. Therefore, we can not reject the null hypothesis that SVG2 model fits the empirical distribution.

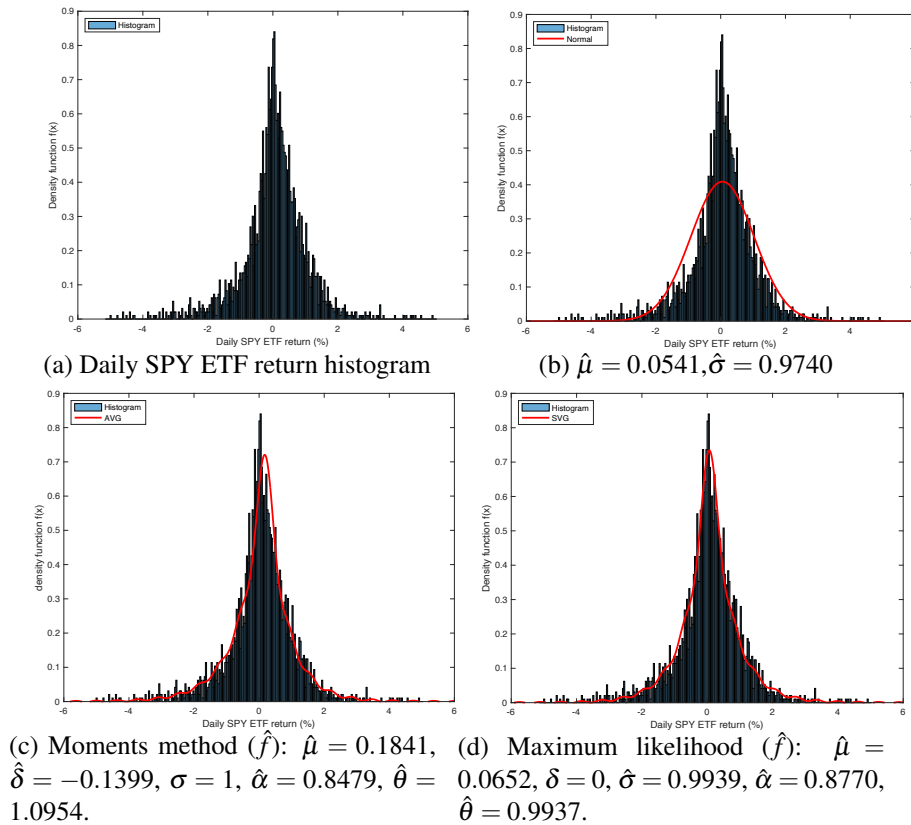


FIGURE 10. Probability density functions for the daily SPY return

The histogram of the daily SPY ETF return was compared to some models in Table 4 as shown in Fig 10. Compare to the CLM in Fig 10b, the peakedness of histogram explains the high level

of the KS-Statistics ($d_n = 0.095791$). But to a lesser extent, the same explanation holds for some AVG models like SVG, AVG1, SVG1 in table 4.

For work related to Normal and exponential distributions, see [35–38]

4. CONCLUSION

The paper explores the use of FRFT based technique as a tool to obtain the probability density function and its derivatives for infinitely divisible distribution. The probability density functions are computed and the distributional proprieties such as leptokurtosis, peakedness, and asymmetry are reviewed for Variance-Gamma (VG) model and Compound Poisson with Normal Compound model. The first and second derivatives of the probability density function of the VG model are also computed in order to build the Fisher information matrix for the Maximum likelihood method.

We perform the maximum likelihood to estimate the Variance Gamma (VG) model with five parameters. The sample data comes from the daily SPY ETF Price data from January 04, 2010 to December 30, 2020. The method of moments and the maximum likelihood were performed on the sample data. Independently of the methods of estimation, the result shows that the VG model provides a better fit than the Classical Lognormal Model (CLM). The Kolmogorov-Smirnov (KS) goodness-of-fit test shows that the maximum likelihood method with FRFT produces a good estimation for the VG model, which fits the empirical distribution of the sample data.

It will be interesting to derive the European option price from the risk-neutral VG model and compare the results with those from the Black-Scholes model.

REFERENCES

- [1] Rama Cont. Empirical properties of asset returns: stylized facts and statistical issues. 2001.
- [2] Wim Schoutens. *Lévy processes in finance: pricing financial derivatives*. 2003.
- [3] L. Mercuri and F. Bellini. Option pricing in a dynamic variance-gamma model. *Derivatives eJournal*, 2010.
- [4] Peter K Clark. A subordinated stochastic process model with finite variance for speculative prices. *Econometrica: journal of the Econometric Society*, pages 135–155, 1973.
- [5] Simon R Hurst, Eckhard Platen, and Svetlozar T Rachev. Subordinated market index models: A comparison. *Financial Engineering and the Japanese Markets*, 4(2):97–124, 1997.
- [6] Dilip B Madan and Eugene Seneta. The variance gamma (vg) model for share market returns. *Journal of business*, pages 511–524, 1990.
- [7] Dilip B Madan and Eugene Seneta. Chebyshev polynomial approximations and characteristic function estimation. *Journal of the Royal Statistical Society: Series B (Methodological)*, 49(2):163–169, 1987.
- [8] Dilip B Madan, Peter P Carr, and Eric C Chang. The variance gamma process and option pricing. *Review of Finance*, 2(1):79–105, 1998.
- [9] Eugene Seneta. Fitting the variance-gamma model to financial data. *Journal of Applied Probability*, pages 177–187, 2004.
- [10] D. Bailey and P. Swarztrauber. A fast method for the numerical evaluation of continuous fourier and laplace transforms. *SIAM J. Sci. Comput.*, 15:1105–1110, 1994.
- [11] David H Bailey and Paul N Swarztrauber. The fractional fourier transform and applications. *SIAM review*, 33(3):389–404, 1991.
- [12] Peter H Westfall. Kurtosis as peakedness, 1905–2014. rip. *The American Statistician*, 68(3):191–195, 2014.
- [13] Achim Klenke. Probability theory. universitext, 2008.
- [14] William Feller. *An introduction to probability theory and its applications, vol 2*. John Wiley & Sons, 2008.
- [15] Francesco Mainardi and Sergei Rogosin. The origin of infinitely divisible distributions: from de finetti’s problem to levy-khintchine formula. *arXiv preprint arXiv:0801.1910*, 2008.

- [16] Maurice George Kendall et al. The advanced theory of statistics. *The advanced theory of statistics.*, (2nd Ed), 1946.
- [17] S James Press. A modified compound poisson process with normal compounding. *Journal of the American Statistical Association*, 63(322):607–613, 1968.
- [18] Paolo Giudici, Geof H Givens, and Bani K Mallick. *Wiley Series in Computational Statistics*. Wiley Online Library, 2013.
- [19] Christophe Chesneau. Sur l’estimateur du maximum de vraisemblance (emv). 2017.
- [20] Brian H Willis, Mohammed Baragilly, and Dyuti Coomar. Maximum likelihood estimation based on newton–raphson iteration for the bivariate random effects model in test accuracy meta-analysis. *Statistical methods in medical research*, 29(4):1197–1211, 2020.
- [21] Anthony William Fairbank Edwards. *Likelihood*. CUP Archive, 1984.
- [22] Leonhard Held and D Sabanés Bové. *Applied statistical inference*, volume 10. Springer, 2014.
- [23] Conall O’Sullivan, Michael Moloney, et al. *The variance gamma scaled self-decomposable process in actuarial modelling*. UCD Centre for Economic Research, 2010.
- [24] Richard Finlay et al. The variance gamma (vg) model with long range dependence. 2009.
- [25] Ahmet Göncü, M Oguz Karahan, and T Umut Kuzubas. Fitting the variance-gamma model: A goodness-of-fit check for emerging markets. *Bogazici Journal of Economics and Administrative Sciences*, 27(2):1–10, 2013.
- [26] Roger L Burford. Shao,” statistics for business and economics”(book review). *Review of Financial Economics*, 3(2):132, 1968.
- [27] Gary King. *Unifying political methodology: The likelihood theory of statistical inference*. Cambridge University Press, 1989.
- [28] George Marsaglia, Wai Wan Tsang, Jingbo Wang, et al. Evaluating kolmogorov’s distribution. *Journal of statistical software*, 8(18):1–4, 2003.
- [29] Frank J Massey Jr. The kolmogorov-smirnov test for goodness of fit. *Journal of the American statistical Association*, 46(253):68–78, 1951.
- [30] Volition Montshiwa, Ntebo Moroke, and Elias Munapo. The efficiency of multiple imputation and maximum likelihood methods for estimating missing values. *Indian Journal of Science and Technology*, 11:1–11, 04 2018.
- [31] Dimitrina S Dimitrova, Vladimir K Kaishev, and Senren Tan. Computing the kolmogorov-smirnov distribution when the underlying cdf is purely discrete, mixed, or continuous. *Journal of Statistical Software*, 95(1):1–42, 2020.
- [32] Vladimir K. Kaishev Dimitrina S. Dimitrova and Senren Tan. *KSgeneral-package: Computing P-Values of the K-S Test for (Dis)Continuous Null Distribution*. R Foundation for Statistical Computing, 10 2020.
- [33] W Krysicki, J Bartos, W Dyczka, K Królikowska, and M Wasilewski. Rachunek prawdopodobieństwa i statystyka matematyczna w zadaniach. *Cz. II. Statystyka matematyczna*, PWN, Warszawa, 1999.
- [34] Magdalena Kucharska and Jolanta Pielaszkiwicz. Nig distribution in modelling stock returns with assumption about stochastic volatility. *Halmstad University*, 2009.
- [35] Aubain Hilaire Nzokem. Sis epidemic model: Birth-and-death markov chain approach. *arXiv preprint arXiv:2102.08992*, 2021.
- [36] Aubain Hilaire Nzokem. *Stochastic and Renewal Methods Applied to Epidemic Models*. PhD thesis, York University , YorkSpace institutional repository, 2020.
- [37] A. Nzokem and N. Madras. Epidemic dynamics and adaptive vaccination strategy: Renewal equation approach. *Bulletin of Mathematical Biology*, 82 9:122, 2020.
- [38] A. Nzokem and N. Madras. Age-structured epidemic with adaptive vaccination strategy: Scalar-renewal equation approach. In *Recent Developments in Mathematical, Statistical and Computational Sciences*. Springer, 2021.

APPENDIX A.1. SOME PROOFS

Proof (2.7):

$$\begin{aligned} f(x_k) &= \frac{1}{2\pi} \int_{-\infty}^{+\infty} \mathcal{F}[f](y) e^{ix_k y} dy \approx \frac{1}{2\pi} \int_{-a/2}^{a/2} \mathcal{F}[f](y) e^{ix_k y} dy = \frac{\gamma}{2\pi} \sum_{j=0}^{n-1} \mathcal{F}[f](y_j) e^{2\pi i(k-\frac{n}{2})(j-\frac{n}{2})\delta} \\ &= \frac{\gamma}{2\pi} e^{-\pi i(k-\frac{n}{2})n\delta} G_k(\mathcal{F}[f](y_j) e^{-\pi i j n \delta}), -\delta) \end{aligned}$$

Proof (2.10) and (3.5)

$$\begin{aligned} \mathcal{F}[f](x) &= E[e^{-ixY_j}] = E(E[e^{-ixY_j}|V_j]) \quad Y_j|_{V_j=v} \sim N(\mu + \delta v, v\sigma^2) \quad \text{and} \quad V_j \sim \Gamma(\alpha, \theta) \\ &= E\left(e^{-ix(\mu + \delta V_j) - \frac{1}{2}\sigma^2 x^2 V_j}\right) = \frac{1}{\Gamma(\alpha)\theta^\alpha} \int_0^{+\infty} v^{\alpha-1} e^{-i(\mu + \delta v)x} e^{-(\frac{1}{2}\sigma^2 x^2 + \frac{1}{\theta})v} dv \\ &= \frac{e^{-i\mu x}}{(\frac{1}{2}\theta\sigma^2 x^2 + 1)^\alpha} E[e^{-i\delta x W}] \quad \text{and} \quad W \sim \Gamma(\alpha, \frac{1}{2}\sigma^2 x^2 + \frac{1}{\theta}) \\ &= \frac{e^{-i\mu x}}{(1 + \frac{1}{2}\theta\sigma^2 x^2 + i\delta\theta x)^\alpha} \end{aligned}$$

Proof (2.13)

$$\begin{aligned} \mathcal{F}[f](x) &= E[e^{-ix\sum_{i=1}^{N(\lambda)} X_j}] = E\left(E[e^{-ix\sum_{i=1}^{N(\lambda)} X_j} | N(\lambda)]\right) \quad N(\lambda) \sim \text{Poisson}(\lambda) \quad \text{and} \quad X_j \sim N(\mu, \sigma^2) \\ &= E\left(E[e^{-ix\sum_{i=1}^k X_j} | N(\lambda) = k]\right) = E\left(E[e^{-ixX_j}]^{N(\lambda)}\right) = e^{\lambda(E[e^{-ixX_j}] - 1)} = e^{\lambda(e^{-i\mu x - \frac{1}{2}\sigma^2 x^2} - 1)} \end{aligned}$$

Proof (3.6):

$$\begin{aligned} \mathcal{F}[f](x) &= \lim_{\theta \rightarrow 0} \frac{e^{-i\mu x}}{(1 + \frac{1}{2}\theta\sigma^2 x^2 + i\delta\theta x)^{\frac{1}{\theta}}} \\ &= e^{-i\mu x} \lim_{\theta \rightarrow 0} e^{-\frac{1}{\theta} \log(1 + \frac{1}{2}\theta\sigma^2 x^2 + i\delta\theta x)} \\ &= e^{-i(\mu + \delta)x - \frac{1}{2}\sigma^2 x^2} \end{aligned}$$

Proof (3.15):

Fourier of the step function

$$u(x) = \begin{cases} 1 & \text{if } 0 \leq x \\ 0 & \text{if } 0 > x \end{cases} \quad \mathcal{F}[u](y) = \frac{1}{iy} + \pi\delta(y)$$

The integral is transformed into convolution of f and u

$$F(x) = \int_{-\infty}^x f(t) dt = \int_{-\infty}^{+\infty} f(\tau) u(x - \tau) d\tau = f(x) * u(x)$$

Using the convolution theorem

$$\mathcal{F}[F](x) = \mathcal{F}[f](x) \mathcal{F}[u](x) \quad \text{and} \quad \mathcal{F}[F](x) = \frac{\mathcal{F}[f](x)}{ix} + \pi\mathcal{F}[f](0)\delta(x)$$

APPENDIX B.2. SECOND ORDER DERIVATIVE OF THE VG DENSITY FUNCTION

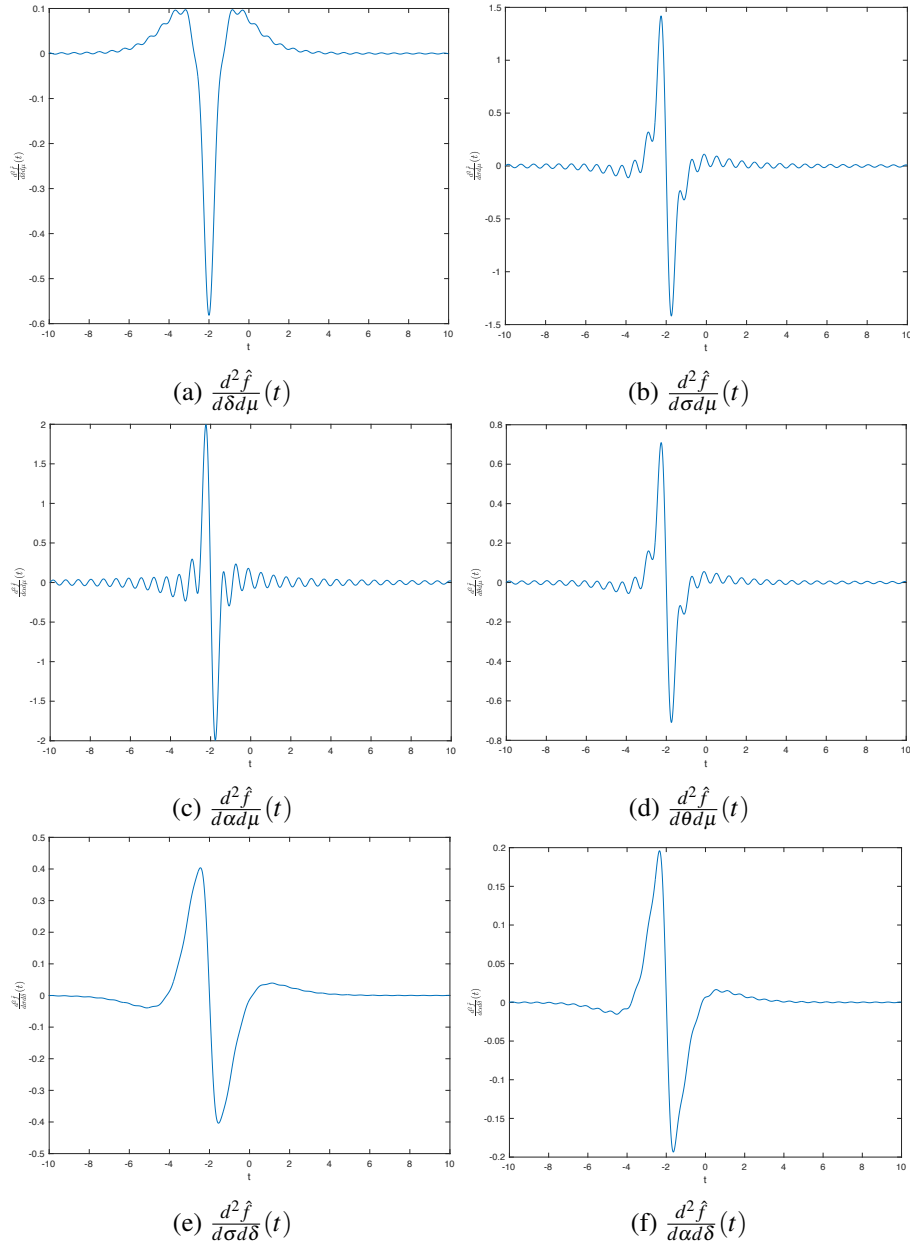


FIGURE 11. Second order derivative of the VG density function with $\mu = -2$, $\delta = 0$, $\sigma = 1$, $\alpha = 1$, $\theta = 1$

APPENDIX C.3. SECOND ORDER DERIVATIVE OF THE VG DENSITY FUNCTION

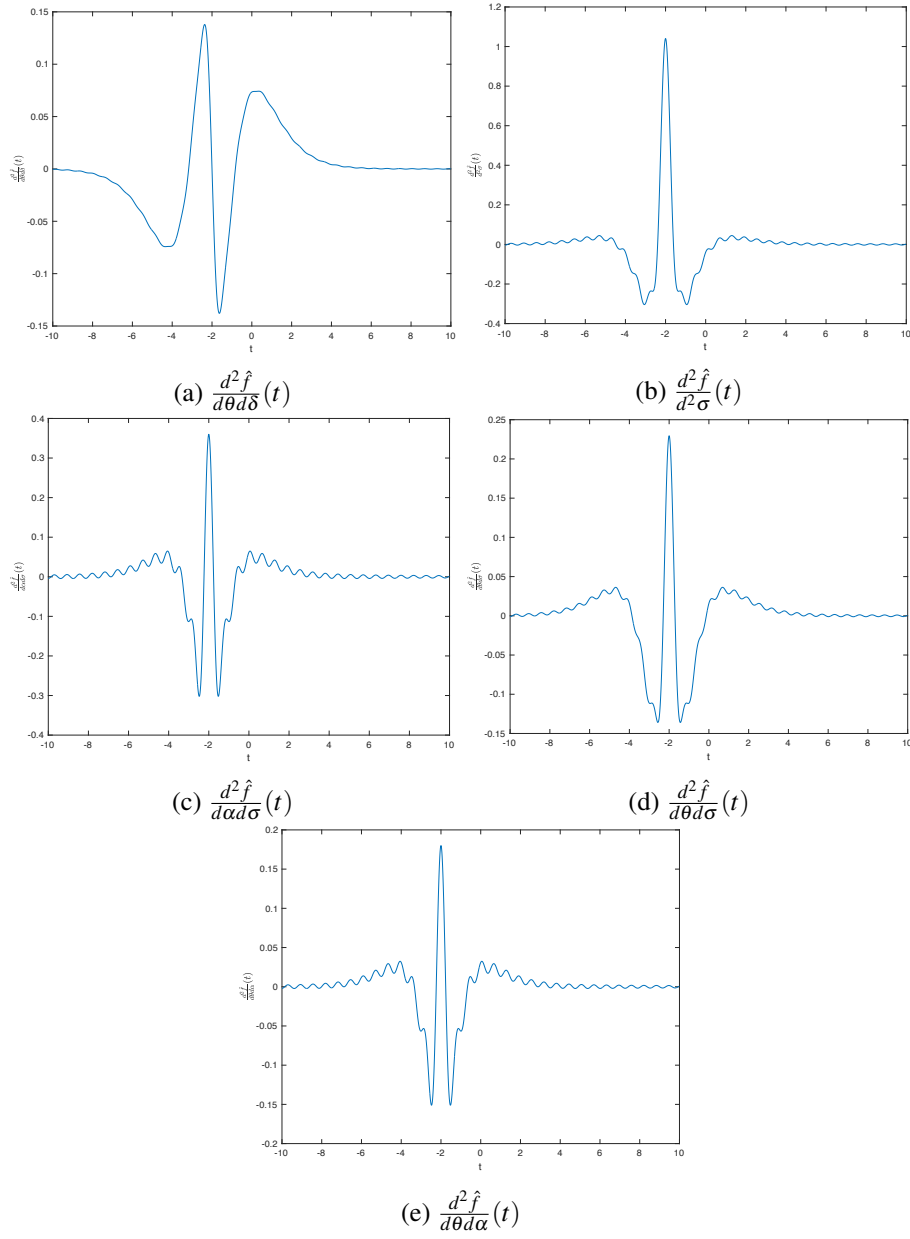


FIGURE 12. Second order derivative of the VG density function with $\mu = -2$, $\delta = 0$, $\sigma = 1$, $\alpha = 1$, $\theta = 1$

APPENDIX D.4. AVG MODEL PARAMETER ESTIMATED
BY NEWTON – RAPHSON ITERATION ALGORITHM (2.23)

TABLE 5. Results of AVG2 Model Parameters Estimations

Iterations	μ	δ	σ	α	θ	$Log(ML)$	$\ \frac{d(Log(ML))}{d(\theta)}\ $
1	0	0	1	1	1	-3582.8388	598.743231
2	0.05905599	-0.0009445	1.03195903	0.9130208	1.03208412	-3561.5099	833.530396
3	0.06949925	0.00400035	1.04101444	0.88478895	1.05131996	-3559.5656	447.807305
4	0.07514039	0.00055771	1.17577397	0.67326429	1.17778666	-3569.6221	211.365781
5	0.08928373	-0.0263716	1.03756321	0.83842661	0.94304967	-3554.4434	498.289445
6	0.08676498	-0.0521887	1.03337015	0.85591875	0.95066351	-3550.6419	204.467192
7	0.086995	-0.0608517	1.02788937	0.87382621	0.95054954	-3549.8465	66.8039738
8	0.08542912	-0.058547	1.02705241	0.88258411	0.94321299	-3549.7023	15.3209117
9	0.08478622	-0.0576654	1.02995166	0.88447791	0.93670036	-3549.6921	1.14764198
10	0.08477798	-0.0577736	1.02922308	0.88449072	0.93831041	-3549.692	0.17287708
11	0.08476475	-0.0577271	1.02960343	0.88450434	0.93755549	-3549.692	0.07850459
12	0.08477094	-0.0577488	1.02942608	0.8844984	0.93790784	-3549.692	0.03723941
13	0.08476804	-0.0577386	1.02950937	0.88450117	0.93774266	-3549.692	0.01732146
14	0.0847694	-0.0577434	1.02947043	0.88449987	0.93781995	-3549.692	0.00813465
15	0.08476876	-0.0577411	1.02948868	0.88450048	0.93778375	-3549.692	0.00380345
16	0.08476906	-0.0577422	1.02948014	0.88450019	0.9378007	-3549.692	0.00178206
17	0.08476892	-0.0577417	1.02948414	0.88450033	0.93779276	-3549.692	0.00083415
18	0.08476898	-0.0577419	1.02948226	0.88450026	0.93779648	-3549.692	0.00039063
19	0.08476895	-0.0577418	1.02948314	0.88450029	0.93779474	-3549.692	0.00018289
20	0.08476897	-0.0577419	1.02948273	0.88450028	0.93779555	-3549.692	8.56E-05
21	0.08476896	-0.0577418	1.02948292	0.88450029	0.93779517	-3549.692	4.01E-05

TABLE 6. Results of SVG2 Model Parameters Estimations

Iterations	μ	σ	α	θ	$Log(ML)$	$\ \frac{d(Log(ML))}{d(\theta)}\ $
1	0	1	1	1	-3582.8388	582.057918
2	0.05883419	1.03172736	0.91367846	1.03172736	-3561.9657	1096.4626
3	0.06789625	1.03903655	0.89847415	1.03903655	-3560.2306	648.976501
4	0.07426127	1.06554771	0.8507772	1.06554771	-3559.7139	270.990173
5	0.07141101	0.86066094	1.14468838	0.86066094	-3567.8236	267.821258
6	0.06686856	0.94781927	0.92720936	0.94781927	-3559.7962	1338.53688
7	0.06739235	0.95934348	0.90760199	0.95934348	-3558.2696	773.42228
8	0.0665979	0.97263343	0.88806105	0.97263343	-3556.6619	428.519657
9	0.06662118	0.98488196	0.87499518	0.98488196	-3555.0979	203.689715
10	0.06614857	0.99253289	0.87413657	0.99253289	-3554.2092	47.3050935
11	0.06523245	0.99394889	0.87669649	0.99394889	-3554.1354	1.62304319
12	0.06515753	0.99386332	0.87702703	0.99386332	-3554.1352	0.00262982
13	0.06515746	0.99386267	0.87702846	0.99386267	-3554.1352	2.69E-08
14	0.06515746	0.99392282	0.87702846	0.99374235	-3554.1352	7.64E-05
15	0.06515746	0.99392282	0.87702846	0.99374236	-3554.1352	2.27E-12

APPENDIX E.5. SVG2 CUMULATIVE FUNCTION (\hat{F}) VERSUS EMPIRICAL FUNCTION (\hat{F}_n), $(1) = |F(\hat{x}_j) - F_n(\hat{x}_{j-1})|$, $(2) = |F(\hat{x}_j) - F_n(\hat{x}_j)|$, $n = 2755$

x_j	$n_{-}(j)$	$F_n(\hat{x}_j)$	$F(\hat{x}_j)$	(1)	(2)	x_j	$n_{-}(j)$	$F_n(\hat{x}_j)$	$F(\hat{x}_j)$	(1)	(2)	x_j	$n_{-}(j)$	$F_n(\hat{x}_j)$	$F(\hat{x}_j)$	(1)	(2)
-5.01	1	0.000362976	0.00053753	0.00053753	0.00017456	-1.685	7	0.04827586	0.0350006	0.01073443	0.01327526	1.64	4	0.96442831	0.95534423	0.00763218	0.00908409
-4.975	0	0.000362976	0.00057061	0.00020763	0.00020763	-1.65	11	0.0522686	0.03665193	0.01162393	0.01561667	1.675	9	0.9676951	0.95760224	0.00682607	0.01009286
-4.94	0	0.000362976	0.00057887	0.00021689	0.00021689	-1.615	3	0.05335753	0.03840489	0.01386372	0.01495264	1.71	4	0.96914701	0.959677	0.0080181	0.00947001
-4.904	0	0.000362976	0.00062067	0.00020267	0.00020267	-1.58	4	0.05480944	0.04030396	0.01305358	0.01450548	1.745	5	0.97096189	0.9615774	0.0075696	0.00938449
-4.87	0	0.000362976	0.00063125	0.00016827	0.00016827	-1.545	5	0.05662432	0.042371	0.01243843	0.01425332	1.78	4	0.97241379	0.96333629	0.0076256	0.0090775
-4.835	0	0.00062976	0.00048258	0.0001196	0.0001196	-1.51	6	0.05880218	0.04462677	0.01199755	0.01417541	1.815	3	0.97350272	0.9649836	0.0073309	0.00851912
-4.8	1	0.000725953	0.00042749	6.45E-05	0.00029847	-1.475	11	0.06279492	0.04708394	0.01171824	0.01571098	1.85	3	0.97459165	0.9665451	0.00695762	0.00804655
-4.765	0	0.000725953	0.00037483	0.00035112	0.00035112	-1.44	8	0.06569873	0.04974601	0.01304891	0.01595272	1.885	2	0.9753176	0.96805709	0.00653456	0.00726051
-4.73	0	0.000725953	0.00033343	0.00039252	0.00039252	-1.405	4	0.06715064	0.05260725	0.01309148	0.01454339	1.92	6	0.97749546	0.96953709	0.00578052	0.00695838
-4.695	0	0.000725953	0.0003106	0.00041499	0.00041499	-1.37	10	0.0707804	0.05566827	0.01149677	0.01512653	1.955	3	0.97858439	0.97100001	0.00649546	0.00758439
-4.66	0	0.000725953	0.00031095	0.0004129	0.0004129	-1.335	6	0.07295826	0.05858677	0.01191413	0.01409199	1.99	3	0.97967332	0.97245259	0.00613181	0.00722074
-4.625	2	0.001451906	0.00034253	0.00038342	0.00110938	-1.3	11	0.076951	0.06222216	0.0107361	0.01472884	2.025	3	0.98076225	0.97389748	0.0057584	0.00686477
-4.59	0	0.001451906	0.00039908	0.00105283	0.00105283	-1.265	5	0.07876588	0.06570024	0.01125076	0.01306564	2.06	1	0.98112523	0.97531775	0.00544451	0.00580748
-4.552	0	0.001451906	0.00047921	0.0009727	0.0009727	-1.23	9	0.08203267	0.06929436	0.00947152	0.0127383	2.095	2	0.98185118	0.97669941	0.00442581	0.00515177
-4.52	1	0.001814882	0.00057667	0.00087523	0.00123821	-1.195	8	0.08493648	0.07297576	0.00905691	0.01196072	2.13	3	0.98294011	0.97803303	0.00381815	0.00490708
-4.485	0	0.001814882	0.00068316	0.00113172	0.00113172	-1.16	16	0.0907441	0.07674627	0.00819021	0.01399783	2.165	3	0.98402904	0.97929655	0.00364536	0.00473249
-4.45	0	0.001814882	0.00078932	0.00102556	0.00102556	-1.125	8	0.09364791	0.08064272	0.01011038	0.01300519	2.2	4	0.98548094	0.98047385	0.00355519	0.00500709
-4.415	2	0.002540835	0.00088588	0.000929	0.00165495	-1.09	7	0.09618875	0.08468243	0.00896548	0.01150631	2.235	1	0.98584392	0.98155588	0.00329506	0.00428804
-4.38	0	0.002540835	0.0009648	0.00157603	0.00157603	-1.055	11	0.10081149	0.08894988	0.00728376	0.0112766	2.27	2	0.98658987	0.98253026	0.00313266	0.00403961
-4.345	0	0.002540835	0.0102027	0.00152057	0.00152057	-1.02	13	0.10490018	0.09357539	0.00682311	0.01154179	2.305	0	0.98693285	0.98339832	0.00317155	0.00353453
-4.31	1	0.002903811	0.00104947	0.00149136	0.00185434	-0.985	11	0.10889292	0.09808268	0.00680391	0.01079665	2.34	1	0.98729583	0.98417215	0.0027607	0.00312368
-4.275	1	0.003266788	0.00105301	0.00118508	0.00221378	-0.95	13	0.11361162	0.10317228	0.00572064	0.01043934	2.375	1	0.9876588	0.98486216	0.00243367	0.00279664
-4.24	0	0.003266788	0.00103485	0.00223193	0.00223193	-0.915	13	0.11833031	0.10865372	0.00497589	0.00969459	2.41	2	0.98838475	0.98548587	0.00212793	0.00289889
-4.205	0	0.003266788	0.00110096	0.00226483	0.00226483	-0.88	15	0.12377495	0.11542697	0.00380334	0.00924798	2.445	1	0.98874773	0.98606329	0.00232146	0.00268444
-4.17	0	0.003266788	0.00096346	0.00230332	0.00230332	-0.845	16	0.12958258	0.1208738	0.00290115	0.00870777	2.48	1	0.98911071	0.98661629	0.00213144	0.00249441
-4.135	0	0.003266788	0.00092963	0.00233716	0.00233716	-0.81	12	0.13393829	0.12768918	0.0018934	0.00624912	2.515	2	0.98938666	0.9871586	0.00195211	0.00267806
-4.1	0	0.003266788	0.00091061	0.00235617	0.00235617	-0.775	18	0.14047187	0.13497076	0.00103247	0.00500111	2.55	2	0.99056261	0.98770945	0.00212721	0.00285317
-4.065	0	0.003266788	0.00091524	0.00235155	0.00235155	-0.74	17	0.14664247	0.14270246	0.00223059	0.00394001	2.585	0	0.99056261	0.98827661	0.00212721	0.00285317
-4.03	0	0.003266788	0.00094992	0.00231686	0.00231686	-0.705	26	0.15607985	0.15085789	0.00421542	0.00522196	2.62	0	0.99056261	0.98886634	0.00169921	0.00169921
-3.995	0	0.003266788	0.00101785	0.00224893	0.00224893	-0.67	21	0.16370236	0.15940559	0.00332573	0.00429677	2.655	1	0.99092529	0.98946709	0.0019552	0.0014585
-3.96	0	0.003266788	0.00111857	0.00214821	0.00214821	-0.635	29	0.17422688	0.16831548	0.00461312	0.0059132	2.69	1	0.99128857	0.99008131	0.00084428	0.00120725
-3.925	0	0.003266788	0.00124789	0.00201388	0.00201388	-0.595	11	0.17967332	0.17440581	0.00337374	0.00210731	2.725	0	0.99128857	0.99069034	0.00059822	0.00059822
-3.89	0	0.003266788	0.00139082	0.00186797	0.00186797	-0.565	32	0.19128857	0.18715116	0.00747784	0.0041374	2.76	1	0.99165154	0.99127971	8.86E-06	0.00037184
-3.855	2	0.00399274	0.00156146	0.00170533	0.00243128	-0.53	21	0.19891107	0.19708652	0.00579795	0.00182455	2.795	0	0.99165154	0.99183768	0.00018632	0.00018632
-3.82	0	0.00399274	0.00172515	0.00226759	0.00226759	-0.495	24	0.2076225	0.2074137	0.00850263	0.0002088	2.83	2	0.9923775	0.99234366	0.00069813	2.78E-05
-3.785	1	0.004355717	0.00187926	0.00211349	0.00247646	-0.46	22	0.21560799	0.21820243	0.01057993	0.00259445	2.865	1	0.99274407	0.99280409	0.00042749	6.45E-05
-3.75	0	0.004355717	0.00201464	0.00234108	0.00234108	-0.425	36	0.22867514	0.22954979	0.01394181	0.00087466	2.9	1	0.99310345	0.99319919	0.00045871	9.57E-05
-3.715	0	0.004355717	0.002212481	0.00223091	0.00223091	-0.39	41	0.24357117	0.24157648	0.01290134	0.00198069	2.935	1	0.99346642	0.9935296	0.00042615	6.32E-05
-3.68	1	0.004718693	0.00206767	0.00214894	0.00251192	-0.355	39	0.25771325	0.25442008	0.01086292	0.00329316	2.97	2	0.99419238	0.99380157	0.00033515	0.00039081
-3.645	0	0.004718693	0.00226154	0.00245715	0.00245715	-0.32	53	0.276951	0.26822579	0.01051254	0.00872521	3.005	0	0.99419238	0.99402611	0.00016626	0.00016626
-3.61	0	0.00508167	0.00229408	0.00242461	0.00278759	-0.285	34	0.2892922	0.28313512	0.00618412	0.00615708	3.04	0	0.99419238	0.99421539	2.30E-05	2.30E-05
-3.575	0	0.00508167	0.0023182	0.00276887	0.00276887	-0.25	41	0.30417423	0.29927354	0.00998135	0.00490069	3.075	1	0.99455535	0.99434827	0.00019199	0.00017099
-3.54	0	0.00508167	0.00232865	0.00275302	0.00275302	-0.215	54	0.32377495	0.31673807	0.01256384	0.00703669	3.11	0	0.99455535	0.99454839	7.07E-06	7.07E-06
-3.505	2	0.005807623	0.00235387	0.0027278	0.00345375	-0.18	52	0.34264973	0.33558577	0.01181081	0.00706396	3.145	0	0.99455535	0.99471239	0.00016604	0.00016604
-3.47	0	0.005807623	0.00240051	0.00340711	0.00340711	-0.145	71	0.36842105	0.35582458	0.01317465	0.01259667	3.18	1	0.99491833	0.99491285	0.0003575	5.48E-06
-3.435	0	0.005807623	0.00247295	0.00332858	0.00332858	-0.11	59	0.38983666	0.37740585	0.00899818	0.01243081	3.215	0	0.99528131	0.99513078	0.00031503	0.00031503
-3.4	3	0.006896552	0.00259707	0.00321056	0.00429949	-0.075	62	0.4123412	0.40022332	0.01038666	0.01211768	3.25	0	0.99528131	0.99537645	9.51E-05	9.51E-05
-3.365	0	0.006896552	0.00275835	0.00413821	0.00413821	-0.04	71	0.43811252	0.42411352	0.01177213	0.0139992	3.285	4	0.99673321	0.99564687	0.00036566	0.000108634
-3.33	0	0.006896552	0.00296233	0.0039342	0.0039342	-0.005	79	0.46678766	0.44889515	0.01074663	0.01792851	3.32	0	0.99673321	0.99593476	0.00079845	0.00079845
-3.295	2	0.007622505	0.00320427	0.00369228	0.0041823	0.03	81	0.49618875	0.47420195	0.00741429	0.0219868	3.355	0	0.99673321	0.99623048	0.00050274	0.00050274
-3.26	0	0.007622505	0.00347555	0.00414695	0.00414695	0.065	66	0.52014519	0.49825099	0.00636334	0.0202931	3.39	1	0.99709619	0.99651915	0.00021407	0.00057704
-3.225	1	0.007985481	0.00376493	0.00385758	0.00422055	0.1	56	0.54047187	0.52503099	0.0053588	0.01496788	3.425	0	0.99			